

Study of the impact of irradiation and temperature on physical and chemical characteristics of paracetamol

Hussein Manaa Ali Al-Maydama¹, Adlia Ahmad Mohammad Abduljabbar²⁺

Abstract

Pure paracetamol samples were subjected to temperature (40 °C) and light (sunlight, UV-lamp, and γ -ray) for time intervals. Treatment impact on the extent of chemical and physical impairments in the treated samples was pursued by comparing the results obtained from thermogravimetric analysis and differential scanning calorimeter (TGA/DSC), scanning electron microscopy (SEM), X-ray diffraction (XRD), high-performance liquid chromatography (HPLC), and photocatalytic decomposition process. Thermal analysis behavior, lifetime prediction, thermal stability, kinetics (i.e., E_a , Z , n), and thermodynamic (ΔG^* , ΔH^* , and ΔS^*) parameters were investigated for samples before and after exposure to heat and light from curves of the non-isothermal gravimetric analysis (TGA) at a heating rate of 10 °C min⁻¹ and with an association of Coats-Redfern and the other standard equations. Changes in crystallinity percentage were calculated relative to the untreated sample using measurements of DSC and XRD. In some treated samples, changes in morphology and purity were observed in SEM images and HPLC results. Kinetic parameters were determined, and the photocatalytic degradation percentage was discussed.

Article History

Received	August 22, 2023
Accepted	May 08, 2024
Published	July 22, 2024

Keywords

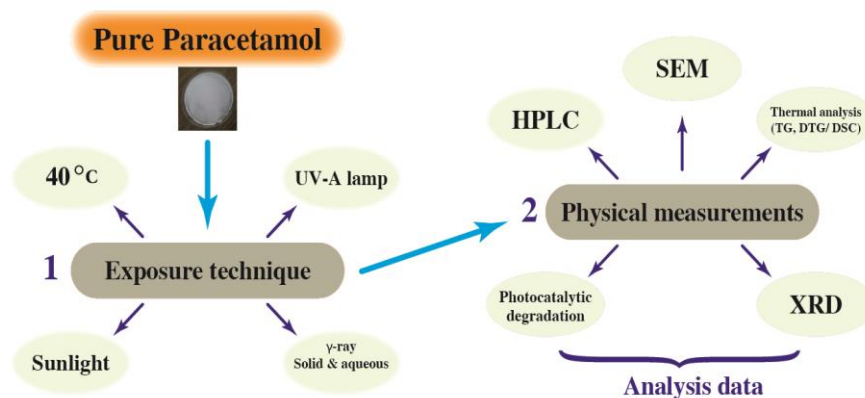
1. Paracetamol;
2. Treatments;
3. TGA/DSC;
4. XRD;
5. SEM.

Section Editor

Irlon Maciel Ferreira

Highlights

- Thermal behavior of paracetamol allows for obtaining thermodynamic data.
- Changes in crystallinity and purity were observed by different techniques.
- Kinetic parameters and photocatalytic decomposition percentage were discussed.



¹Sana'a University, Faculty of Science, Sana'a, Yemen. ²Amran University, Faculty of Applied Sciences and Humanities, Amran, Yemen.

+Corresponding author: Adlia Ahmad Abduljabbar. Phone: +967736966503. Email address: dr.adlia@amu.edu.ye

1. Introduction

The chemical changes, physical state, or form, of Active Pharmaceutical Ingredients (API), as well as other performance characteristics of pharmacological products (such as dissolution, particle changes, and surface modifications), all have a substantial impact on product efficacy and safety (Huynh-Ba, 2010). The efficacy, safety, and quality of pharmaceutical products may be affected by various environmental factors, particularly those distributed in harsh climates or entering commerce abroad. Most environmental impact factors on stability are caused by insufficient storage (in heat, moisture, or sunlight), which can cause the medicine to degrade and lose its therapeutic properties (Akyar, 2011).

Acetaminophen, often known as paracetamol, is a popular analgesic and antipyretic used to treat fever and acute pain. Some studies (Lusina *et al.*, 2005) focused on how the characteristics of analgesics varied when exposed to normal and accelerated conditions (above 50 °C and 80% relative humidity). The studies that documented the decomposition of analgesics caused by radiation impacts were greatly improved, and each of these studies addresses the impact of long-term storage conditions (2 weeks - 3 months) (Suno *et al.*, 2015; Vermeire and Remon, 1999). In our paper published elsewhere (Al-Maydama *et al.*, 2018), such changes have been observed in the treated Aspirin samples by sunlight, UV-lamp, and γ -ray when compared with the untreated one.

When thermally evaluated utilizing single and multiple heating rates techniques with a change in its heat of fusion value, the thermal degradation of the paracetamol study was previously a topic of interest (Oliveira *et al.*, 2017; Schnitzler *et al.*, 2002; Tomassetti *et al.*, 2005). Studies on the photocatalytic degradation of the analgesics (paracetamol) under investigation were conducted using UV and sunlight systems in the presence of TiO₂, and their efficacy was dependent on the intensity of the light (Aguilar *et al.*, 2011; Méndez-Arriaga *et al.*, 2008; Moctezuma *et al.*, 2012; Trujillano *et al.*, 2022). The described photocatalytic decomposition studies utilized different methodologies and aspects than this work.

In this work, the analgesic acetaminophen (paracetamol) has been exposed to temperature (40 °C) and irradiation (sunlight, UV-lamp, and γ -ray) to observe their effects. The purpose of this study is to investigate how temperature and irradiation affect the chemical and physical properties of paracetamol. To determine the purity, crystal properties, and decomposition of both treated and untreated paracetamol samples, various techniques such as high-performance liquid chromatography (HPLC), X-ray diffraction (XRD), scanning electron microscopy (SEM), thermal analysis, and photocatalytic degradation were used.

The thermal analysis behavior, lifetime prediction, decomposition kinetics, and thermodynamic parameters from a single heating rate (10 °C min⁻¹) using a technique of the non-isothermal thermogravimetric analysis (TG/DTG) and differential scanning calorimeter (DSC) were processed by the Coats-Redfern (CR) method (Coats and Redfern, 1964) with the assistance of relevant standard equations. The chemical or physical changes due to temperature and irradiation exposure were compared to the results of the standard sample (untreated) obtained from the relevant measurements of the study and hence discussed.

2. Experimental

2.1. Reagents and solutions

The Modern Pharmaceutical Company (Yemen) provided the analytical standard grade ($\geq 99\%$) paracetamol compound for use in pharmaceutical products (also known as acetaminophen). Chemicals suitable for HPLC such as methanol and water, are offered by Sharlua. 99% purity of TiO₂ (anatase) is available from Sigma-Aldrich.

According to the British Pharmacopeia (2009), paracetamol has the following structure and physical characteristics.

Acetaminophen (paracetamol)

Acetamide, N-(4-hydroxyphenyl)-4'-Hydroxyacetanilide

M.Wt: 151.16 g mol⁻¹

Chemical Formula: C₈H₉NO₂

M.P.: 168–172 °C

2.2. Preparing sample

2.2.1. Exposure strategy

A specific quantity of the standard paracetamol took place over 8 days in vials at a temperature of 40 °C in a digital oven (Memert GmbH Co. KG, Germany). A nearly identical amount of the pharmaceutical was exposed to a 300 W UV-A lamp ($\lambda=365$ nm) for 12 h at far from 18 cm. Approximately the same amount of the drug was exposed to sunlight for 8 days. A total of 80 Gy of γ -ray radiation (source Co⁶⁰) was administered to two Petri plates, each of which contained an equal amount of solid and aqueous samples of paracetamol.

2.2.2. Sampling for photocatalytic study

The sunlight photocatalytic decomposition of the samples of standard and treated paracetamol was conducted by combining 20 ppm of the sample with 1 mg mL⁻¹ aqueous solution of TiO₂ catalyst (anatase- purity 99%, Sigma-Aldrich) to make up a reacting mixture. A 300-minute direct sunlight exposure of 15 min time intervals per aliquot collection was considered. Therefore, for each paracetamol sample, fifteen samples of 25 mL reacting mixture were prepared to correspond to the consecutive 15 min time intervals each individually. The samples were exposed to sunlight in open beakers on a sunny day from 10:00 am to 2:00 pm (winter). An aliquot of 10 mL of the reaction mixture was placed into a covered test tube at every consecutive 15 min interval of sunlight exposure and centrifuged to separate the catalyst residue for 30 min (4000 r.p.m.). The pH of the solution used in the photocatalytic experiment was measured at 6.5. At the same concentration of the interest of paracetamol samples, the photocatalytic decomposition processes were individually investigated.

2.3. Methods and physical measurements

2.3.1. Thermal analysis

The TGA and DSC curves of paracetamol-treated and untreated were analyzed using non-isothermal Netzsch, STA 449 F3. All measurements employed highly sintered Al₂O₃ as a reference material and sample masses ranging from 6.4 to 9.2 mg. The samples under investigation were subjected to thermal

analysis measures at a heating rate of $10\text{ }^{\circ}\text{C min}^{-1}$, nitrogen flow rates of 25 mL min^{-1} , and temperature ranges of $25\text{--}650\text{ }^{\circ}\text{C}$.

The relevant TGA curves were used to derive quantitative data. The kinetic parameters of the decomposition processes before and after treatments were calculated using the Coats-Redfern method (Coats and Redfern, 1964).

2.3.2. X-ray diffraction

The instrumentation, Shimadzu ED-720 XD-2 powder X-ray diffractometer at 20 mA current and a voltage of 35 kV with a CuK(U) radiation generator at $1^{\circ}\text{ min}^{-1}$ scanning rate in the range of $5^{\circ} < 2\theta < 65^{\circ}$ and a wavelength of 1.54056 \AA was used to obtain the powder X-ray diffraction patterns of the paracetamol samples.

2.3.3. High-performance liquid chromatography (HPLC)

For separation and detection of paracetamol, the HPLC system (HPLC Jasco, UV2075 UV/Vis detector, and Pump 2089 plus) was employed. The mobile phase was a 30:70 mixture of methanol and water. Before and after treatments, 100 mg of paracetamol samples were dissolved in 100 mL of the mobile phase. 10 mL of this solution was diluted with the mobile phase to a concentration of 0.1 mg mL^{-1} . At room temperature ($25\text{ }^{\circ}\text{C}$), the analysis was performed at a flow rate of 2 mL min^{-1} .

The BDS Hypersil C18 column ($200\text{ mm} \times 4.6\text{ mm}$) was employed. A UV-visible detector was used to record chromatograms at 245 nm, and the retention time ranged from 5.27 to 5.33 min.

2.3.4. Scanning electron microscope (SEM)

The surface morphology and form of the particles were examined using a scanning electron microscope. Using an instrumental Jeol Jem-1200 EX II electron microscope and gold-coated samples, SEM pictures took place at a 20 kV acceleration voltage.

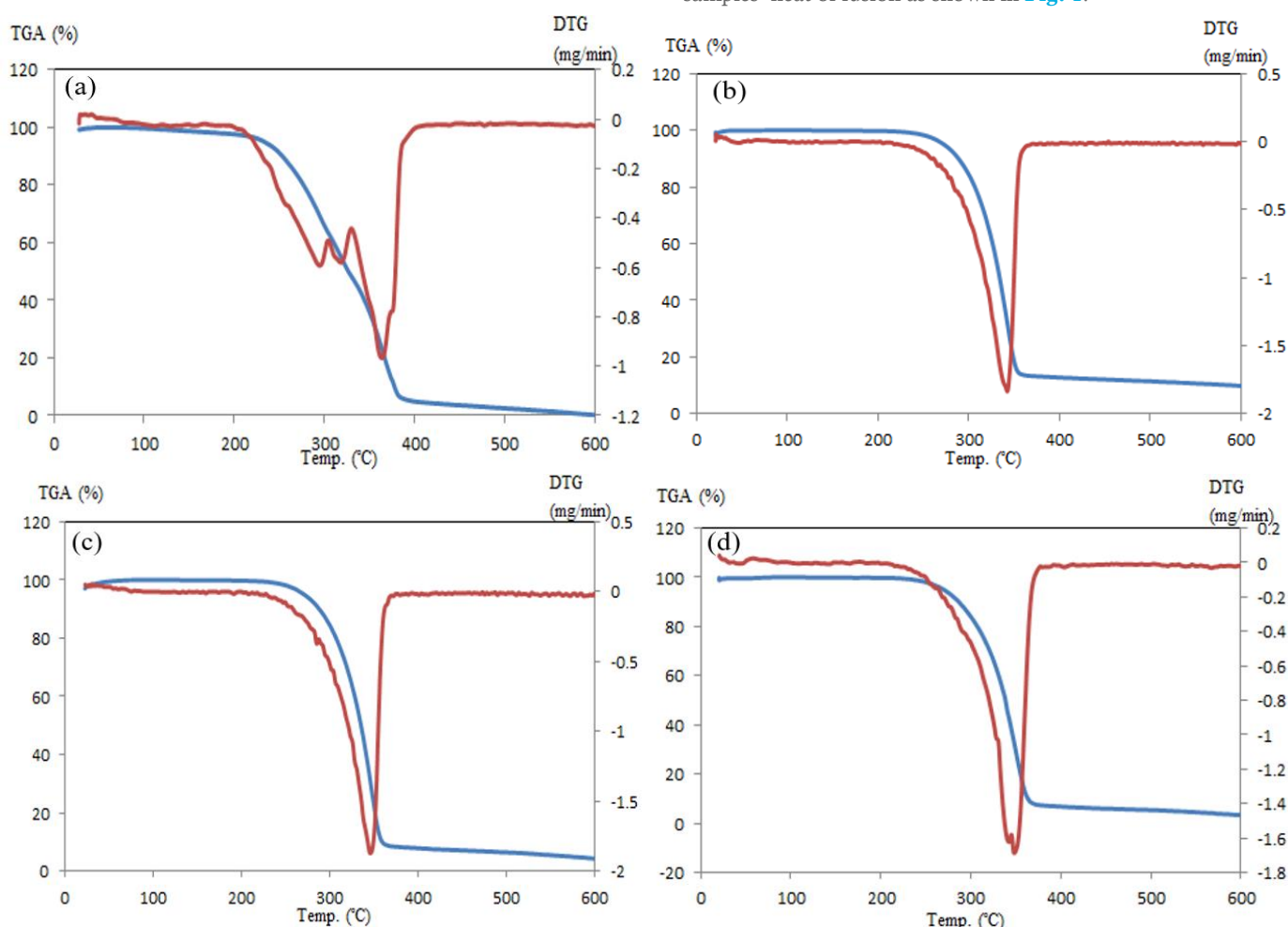
2.3.5. Electronic spectra

The absorbance of the treated and untreated paracetamol was measured at various time intervals for the photocatalytic decomposition using a UV-VIS Spectrophotometer (Specord200, Analytik Jena). Paracetamol has maximum absorbance (λ_{max}) at 254 nm. The Beer-Lambert law was applied to compute the relevant data at λ_{max} from the electronic spectra curves.

3. Results and discussion

3.1. Thermal analysis of paracetamol

The TG and DTG curves recorded for the paracetamol before and after treatments are shown in Fig. 1. These curves describe and evaluate the thermal decomposition behavior of paracetamol samples at a given experimental condition. The results of the thermal degradation behavior of these samples are summarized in Table 1. It is noteworthy that the DSC curves in Fig. 2 exhibit a prominent single endothermic peak for all paracetamol samples almost within the range of their single degradation steps. These endothermic peaks are attributed to the samples' heat of fusion as shown in Fig. 1.



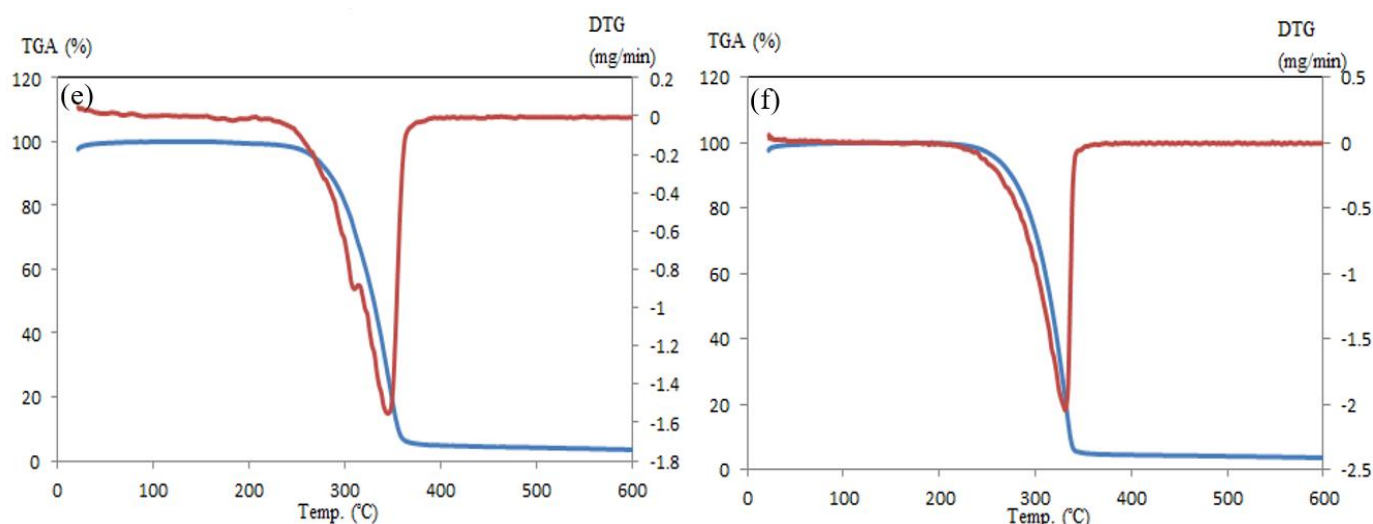


Figure 1. TG and DTG curves of paracetamol before and after treatments (a) standard, (b) 40 °C-8d, (c) UV-12 h, (d) γ -solid, (e) γ -aq, (f) Sun-8d.

Table 1. Thermodynamic and kinetic parameters of thermal decomposition of the paracetamol samples before and after exposure to irradiation and temperature.

Paracetamol samples	Step	n	E_a kJ mol ⁻¹	TGA			$\log Z$ at T_{DTG}	Δm %	ΔG^* kJ mol ⁻¹	ΔH^* kJ mol ⁻¹	ΔS^* kJ mol ⁻¹	Final residue
				T_i °C	T_f °C	T_{DTG} °C						
Standard	1	3.6	126.2	211.1	398.2	354.1	11.16	95	144	121	-37.5	5%
40 °C-8d	1	0.7	118.4	227.8	360.2	338	9.74	86.2	152.7	113.3	-64.5	13.8%
UV-12h	1	0.75	111.3	227.8	367.5	345.3	9.04	91.3	154.4	106.2	-78	8.7%
γ -solid	1	0.7	104.7	232.7	372.5	342.9	8.39	92.3	155.2	99.54	-90.3	7.7%
γ -aqueous	1	1.1	122.3	230.2	370.1	340.5	10.16	94.4	151.8	117.2	-56.4	5.6%
Sunlight-8d	1	0.6	116.8	221.1	344.1	326.8	9.82	94.5	149.4	111.8	-62.7	5.5%

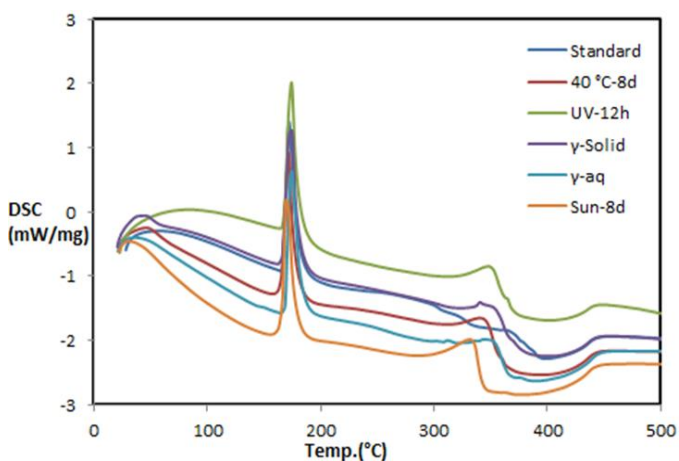


Figure 2. DSC profiles of the paracetamol samples before and after exposure to irradiation and temperature.

3.1.1. Assessment of thermal decomposition kinetics

The activation energy (E_a) and pre-exponential factor (Z) are calculated using the CR method (Coats and Redfern, 1964) for the proper order of reaction (n) to assess the decomposition of the thermal kinetics parameters at (10 °C min⁻¹) single heating rate. The Coats-Redfern equation is linearized for a well-selected order of reaction, and the activation energy (E_a) is determined from the slope of Eqs. 1 and 2:

$$\log \frac{1-(1-\alpha)^{1-n}}{T^2(1-n)} = \log \left[\frac{ZR}{qE_a} \left(1 - \frac{2RT}{E_a} \right) \right] - \frac{E_a}{2.303RT} \quad \text{for } n \neq 1 \quad (1)$$

$$\log \left[\frac{-\log(1-\alpha)}{T^2} \right] = \log \left[\frac{ZR}{qE_a} \left(1 - \frac{2RT}{E_a} \right) \right] - \frac{E_a}{2.303RT} \quad \text{for } n = 1 \quad (2)$$

where: T = temperature (K), α = fraction of weight loss, Z = pre-exponential factor, q = heating rate, n = order of reaction, and R = molar gas constant.

For a temperature of maximum mass loss rate (T_{DTG}), the pre-exponential factor (Z) is computed from the intercept. In general, one step of the decomposition process for the samples of standard and treated paracetamol can be seen by attentively examining the TG/DTG curves (Fig. 1).

3.1.2. Thermal decomposition behavior of paracetamol

The thermal studies of paracetamol at single and multiple heating rates were mentioned elsewhere (Schnitzler *et al.*, 2002; Tomassetti *et al.*, 2005). It showed a single-step (214–357 °C) degradation behavior at a T_{DTG} peak at 326 °C with various heat of fusion values (22.8–35.7 kJ mol⁻¹). This agrees fairly with the results obtained for the samples with interest. Unlike the treated samples, although the TG curve of the untreated paracetamol sample shows one degradation step, its DTG curve appears with two immature peaks followed by one principal peak at 354.1 °C. This may indicate rate variation due to competitive degradation reaction. The standard paracetamol (untreated sample) loses 95% in a single step at 211.1 – 398.2 °C at a maximum temperature (T_{DTG}) of 354.1 °C and 5% residue. According to the order of reaction ($n = 3.6$), the activation energy is determined to be 126.2 kJ mol⁻¹. The parameters of thermodynamic ΔH^* , ΔS^* , and

ΔG^* are 121 kJ mol⁻¹, -37.5 J K⁻¹ mol⁻¹, and 144.6 kJ mol⁻¹, respectively.

For paracetamol exposed to 40 °C temperature, the single step (227.8 – 360.2 °C) at T_{DTG} of 338 °C is accompanied by a mass loss of 86.2% and 13.8% residue. The activation energy E_a for the single step ($n = 0.7$) is 118.4 kJ mol⁻¹ and the thermodynamic parameters (ΔH^* , ΔS^* , and ΔG^*) calculated for this step are -113.3 kJ mol⁻¹, -64.5 J K⁻¹ mol⁻¹, and 152.7 kJ mol⁻¹, respectively.

The UV-lamp irradiated paracetamol shows a single step of degradation (227.8 – 367.5 °C) at T_{DTG} of 345.3 °C with mass loss of 91.3% and residue of 9.7%. The value of activation energy of the single ($n = 0.75$) step is 111.3 kJ mol⁻¹ and the values of ΔH^* , ΔS^* , and ΔG^* of this step are 106.2 kJ mol⁻¹, -78 J K⁻¹ mol⁻¹, and 154.4 kJ mol⁻¹, respectively.

The single degradation steps of the treated paracetamol with γ -ray in solid and aqueous states are observed at (232.7 – 372.5 °C) and (230.2 – 370.1 °C) range at T_{DTG} of 243.9 °C and 340.5 °C with mass losses of 92.3% and 94.4%, and residues of 7.7% and 5.6%, respectively. Values of E_a , ΔH^* , ΔS^* , and ΔG^* for the single decomposition step of paracetamol irradiated with γ -ray in solid ($n = 0.7$) and aqueous ($n = 1.1$) states are (104.7 kJ mol⁻¹, 99.5 kJ mol⁻¹, -190.3 J K⁻¹ mol⁻¹, and 155.2 kJ mol⁻¹) and (122.3 kJ mol⁻¹, 117.2 kJ mol⁻¹, -56.4 J K⁻¹ mol⁻¹, and 151.8 kJ mol⁻¹), respectively.

The degradation of paracetamol treated with sunlight shows single-step (221.1 – 344.1 °C) at T_{DTG} of 326.8 °C with mass loss of 94.5% and residue of 5.5%. The activation energy for the single ($n = 0.6$) step is found to be 116.8 kJ mol⁻¹. The values of ΔH^* , ΔS^* , and ΔG^* are 111.8 kJ mol⁻¹, -62.7 J K⁻¹ mol⁻¹, and 149.4 kJ mol⁻¹, respectively.

Typically, for all the samples, the positive values of ΔH^* and ΔG^* for the transition-state reaction indicate an extremely small equilibrium constant and the reactants are stable concerning

the formation of the activated complex and there are insignificant variations in values of the samples before and after treatments. The changes in activation entropy values for the individual steps of the paracetamol samples' decomposition are negative, reflecting the corresponding reduction in degrees of freedom for rotation in the reactants and generating the new degrees of freedom for vibration in the activated complex, which is more ordered than the reactants (Al-Maydama, 2004).

3.1.3. Estimating the lifetime (tf)

From the TGA observed curves for the paracetamol samples before and after treatments, the lifetime was estimated for various temperatures (25, 40, 100, 150, and 200 °C). The estimated lifetime of the paracetamol samples can be defined as the time when 5% of the degradation was reached (Prime *et al.*, 2009), and for $n \neq 1$ be obtained from the Eq. 3:

$$t_f = \frac{(1-0.95^{1-n})}{Z(1-n)} \exp \frac{E_a}{RT} \quad (3)$$

According to the data for kinetics collected by applying the CR method (Tables 1 and 2) and Eq. 3, the predicted lifetime for the decomposition of the paracetamol samples at a conversion of 5% and a variety of temperatures are summarized in Table 2. Values of the estimated lifetime for the decomposition vary consistently with the temperatures of (25, 40, 100, 150, and 200 °C). A lifetime ($t_{5\%, 25^\circ\text{C}}$) is typically estimated using the time for 5% conversion of the samples of treated and untreated paracetamol at 25 °C (Prime *et al.*, 2009). All the samples show almost the same lifetime except for the value (4.7×10^8 s) of γ -ray in the solid state, as given in Table 2.

Table 2. The standard and treated paracetamol samples' DSC characteristics and calculated values of a lifetime at different temperatures of the decomposition based on weight loss ($\alpha = 5\%$).

Variable	DSC			t_f (sec) at 5% conversion					Log Z at 5%
	M.P. (°C)	ΔH_f kJ mol ⁻¹	X _c (%)	25 °C	40 °C	100 °C	150 °C	200 °C	
Standard	171.5	18.9	100	5.1×10^9	4.4×10^8	1.8×10^5	1.5×10^3	33.3	11.15
40 °C-8d	154.5	15.3	81	5.2×10^9	5.3×10^8	3.5×10^5	3.9×10^3	110.1	9.74
UV-12h	174.5	19.5	103.1	1.6×10^9	1.8×10^8	1.9×10^5	2.7×10^3	93.6	9.03
γ -solid	174.7	19.8	104.7	4.7×10^8	6.1×10^7	9.5×10^4	1.8×10^3	75.8	8.39
γ -aqueous	174.5	19.1	100.9	9.9×10^9	9.3×10^8	4.8×10^5	4.6×10^3	115.4	10.16
Sunlight-8d	169.2	17	90.02	2.3×10^9	2.4×10^8	1.8×10^5	2.1×10^3	61.4	9.82

3.1.4. Thermal stability of paracetamol

Based on temperature fluctuation at the maximum degradation rate (T_{DTG}), the thermal stability of decomposition is measured (Al-Maydama *et al.*, 2009; Donia *et al.*, 1992). As the paracetamol samples before and after treatments show almost incomparable differences in their temperature of the maximum degradation rates (T_{DTG}) the increase in thermal stability of the paracetamol samples can be listed in the following order:

Standard (354.1 °C) > UV-sample (345.3 °C) > γ -solid (342.9 °C) > γ -ray-aqueous (340.5 °C) > 40 °C-sample (338 °C) > sunlight (326.8 °C).

The decomposition rate consequently decreases as the slope of the CR method plot increases because the activation energy increases. It follows that the activation energies (kJ mol⁻¹)

of the treated and untreated paracetamol samples rise in the following order:

Standard (126.2) > γ -ray-aqueous (124.1) > 40 °C-sample (120.4) > sunlight (116.8) > UV-sample (111.3) > γ -solid (104.7).

Consequently, the decomposition rates are increasing in the following order:

γ -solid > UV-sample > sunlight > 40 °C-sample > γ -aqueous > Standard

3.1.5. DSC technique

The curves of DSC for the treated and untreated paracetamol samples are shown in Fig. 2. According to the DSC curves, the melting point of the standard paracetamol is 171.5 °C

which agrees with the literature values of 168 – 172 °C, indicating the extremely pure of the standard paracetamol (British Pharmacopeia, 2009). The results indicate that when the melting points of the standard paracetamol and the treated samples are compared, the melting point of the paracetamol exposed to sunlight (169.2 °C) is within the range of values reported in the literature, while that exposed to 40 °C exhibits the lowest melting point value (154.5 °C). However, the melting points of paracetamol treated with UV-lamp and γ -ray in solid and aqueous states (174.4 – 174.8 C) are noticeably higher than the literature values. Various fusion heat values (22.8 – 35.7 kJ mol⁻¹) were reported for paracetamol (Oliveira *et al.*, 2017; Schnitzler *et al.*, 2002; Tomassetti *et al.*, 2005). Some of these values are fairly comparable to the value obtained (18.9 kJ mol⁻¹) for the untreated sample.

The ratio of the treated paracetamol sample's enthalpy of fusion to that of the standard paracetamol was applied to determine the relative crystallinity of the treated paracetamol samples (i.e., 40 °C, UV, sunshine, and -ray) as given in the Eq. 4:

$$X_c(\%) = \frac{\Delta H_f}{\Delta H_f^0} \times 100 \quad (4)$$

where X_c is the relative crystallinity, ΔH_f is the enthalpy of fusion for the treated sample and ΔH_f^0 is that of the 100 % crystalline standard, i.e., of the standard paracetamol sample.

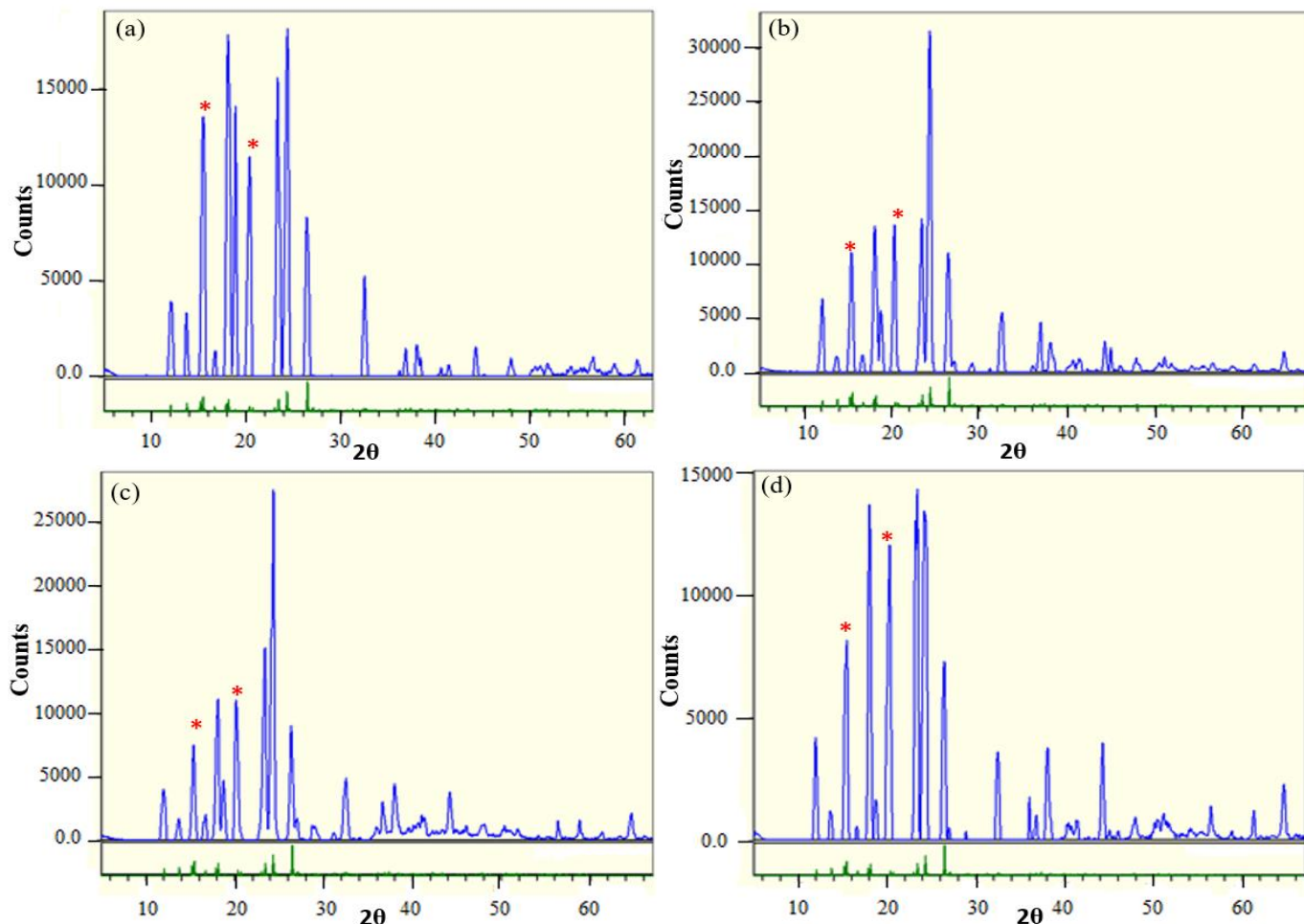
The relative crystallinity and fusion heat of the standard and treated paracetamol samples were evaluated using Eq. 4, as given in Table 2. When compared to the greatest crystallinity value (100%) estimated for the standard paracetamol, the treated

paracetamol samples' extent of crystallinity reduction is measured (Varshny and Patel, 1994).

The lowest values of the relative crystallinity (81 and 90%) and consequently that of the enthalpy of fusion (15.3 and 17 kJ mol⁻¹) are reported for the paracetamol samples exposed to the temperature of 40 °C and sunlight, respectively.

3.2. X-ray diffraction

Figure 3 displays the paracetamol XRD patterns before and after being exposed to radiation and temperature. These patterns demonstrate that paracetamol has a polycrystalline phase (five principal peaks at $15^\circ \leq 2\theta \leq 45.5^\circ$). Comparing the apparent sublattice peaks with the crystallographic data available in the crystallographic information file no: 2103465. cif, the crystal structures of all paracetamol samples except sunlight-treated samples belong to the orthorhombic symmetry, space group Pbc_a. While the XRD pattern of the sunlight-treated paracetamol sample matches essentially with the monoclinic symmetry, space group *P2*/*a* (Druzbin *et al.*, 2015; Jendrzejewska *et al.*, 2020), mixed with the original orthorhombic polymorph as a minor component. The occurrence of some crystal lattice inversion for the paracetamol samples treated with UV, γ -ray both solid and aqueous states, and at 40 °C, can be evidenced by the interchange of relative intensities of the sublattice peaks observed at $2\theta \sim 15^\circ$ and $\sim 20^\circ$, as indicated by asterisks (*) in the relevant patterns. This crystallographic inversion represents one of some lattice disorders, as expected from DSC results, particularly those samples treated with sunlight and at 40 °C, behind which both ΔH_f and M.P. are greatly dropped.



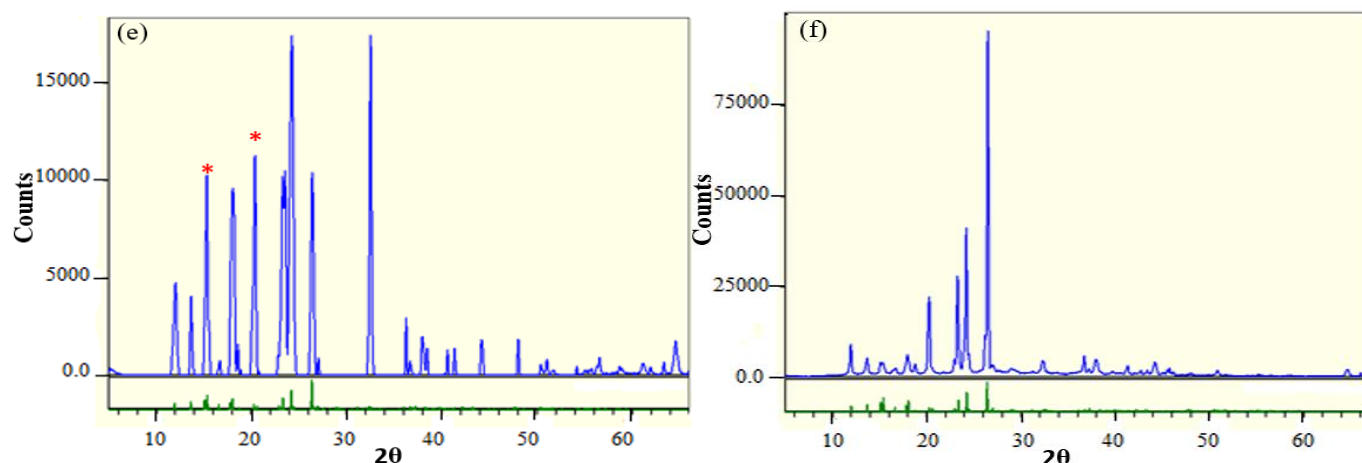


Figure 3. XRD patterns for paracetamol before and after exposure to irradiation and temperature: (a) standard, (b) 40 °C-8 d, (c) UV-12 h, (d) γ -solid, (e) γ -aq, (f) Sun-8 d.

Source: Elaborated by the authors using data from MDI Jade 5.

The Debye-Scherrer and Williamson-Hall (W-H) Eqs. 5 and 6 can be used for calculating the average crystal size (Yousaf *et al.*, 2021):

$$D = \frac{k\lambda}{\beta_{hkl} \cos \theta} \quad (5)$$

$$\beta_{hkl} \cos \theta = \frac{k\lambda}{D} + 4\varepsilon \sin \theta \quad (6)$$

where β is full width at half maximum (FWHM in radians), λ is the wavelength ($\lambda=1.54056$ Å), D is the particle size (nm), k is

Scherer constant (0.94), and θ is the diffraction angle, and ε is the micro strain.

The slope of the fitted line indicating the strain can be used to calculate the effective particle size.

Table 3 shows a comparison of the particle size of paracetamol samples using Scherrer and Williamson-hall (W-H) equations. Due to variation in averaging particle distribution, the values of the average crystalline size gained for the W-H equation showed significant fluctuation. The crystalline size (10.34-57.93 nm) that was observed for the W-H equation is inconsistent with Scherrer's equation.

Table 3. The properties of lattice crystalline and relative purity of the standard and treated paracetamol samples using XRD and HPLC techniques.

Paracetamol samples	HPLC Purity%	2θ	β	XRD		Microstrain	$X_c\%$
				D (nm)			
				Scherrer	W-H		
Standard	100	15.46	0.006178	23.54	28.39	0.0009	100
		18.08	0.006754				
		23.32	0.005917				
		24.36	0.006423				
		26.38	0.006126				
40 °C-8d	98.7	15.4	0.006388	22.61	24.54	0.0004	113.8
		18.06	0.006999				
		23.42	0.006423				
		24.3	0.006301				
		26.42	0.006562				
UV-12h	98.9	15.36	0.005864	23.78	26.33	0.0007	93.9
		18.1	0.006754				
		23.4	0.006545				
		24.34	0.005969				
		26.34	0.005986				
γ -solid	101.4	15.48	0.006353	20.32	57.93	0.0068	99.4
		18	0.005655				
		23.4	0.011083				
		24.38	0.009809				
		26.44	0.006144				
γ -aqueous	101.3	15.32	0.00473	23.75	42.59	0.0037	83.9
		18.06	0.006632				
		23.54	0.010489				
		24.24	0.006597				
		26.4	0.005096				
Sunlight-8d	99.5	15.099	0.008255	24.08	10.34	-0.01	126.5
		17.959	0.006266				
		23.279	0.003857				
		24.201	0.003665				
		26.48	0.003019				

According to the integrated areas of the five principal peaks as a ratio to those of the standard samples, crystallinity calculation is given in **Table 3**. According to the results reported in **Table 3**, paracetamol treated with γ -ray in the aqueous state (83.9%) and with UV light (93.9%) significantly decreased crystallinity. The nanoparticle size in the literature ranges between 1-100 nm (Boverhof *et al.*, 2015). The particle size obtained from XRD (**Table 3**) for the untreated sample is 23.54 nm. The particle size of treated paracetamol samples calculated by XRD exhibits no effects on their size of nanoparticles (20.3 – 24.08 nm) due to radiation and temperature treatments. This means that, as the particle size depends only on the crystallinity degree and phase transformations, it seems that the treatments of the samples were not able to affect the bulk of particles.

3.3. High-performance liquid chromatography (HPLC) analysis

Typical chromatograms of HPLC for the paracetamol samples' purity analyses are shown in **Fig. 4**, and all samples were analyzed using the British Pharmacopoeia standard method. HPLC profiles of the samples of standard and treated paracetamol have a ranging retention time (R_f) of (5.27 – 5.33 min). The insignificant changes in the absolute purity values determined by HPLC are due to the absence of chemical changes in the composition of the paracetamol samples. Nevertheless, no unusual peaks in HPLC chromatograms of the paracetamol-treated samples are seen under the studied conditions. In general, the results in **Table 3** show no significant changes in the purity of the paracetamol exposed to temperature and radiation.

However, under the investigated circumstances there are no unexpected peaks in the HPLC chromatograms of the treated samples of paracetamol. The results in **Table 3** generally demonstrate no appreciable variations in the purity of the paracetamol subjected to heat and radiation.

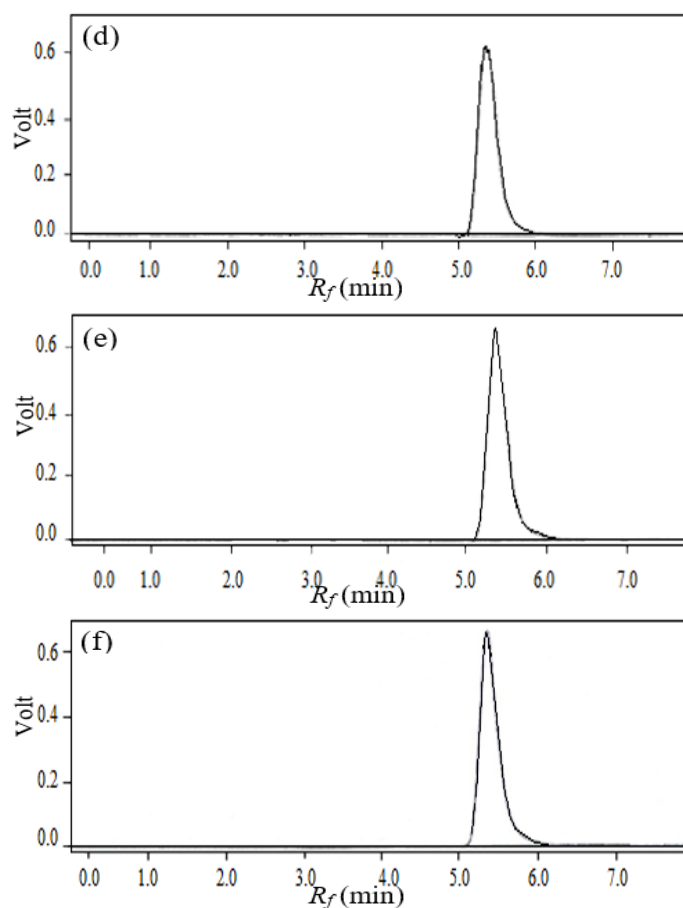
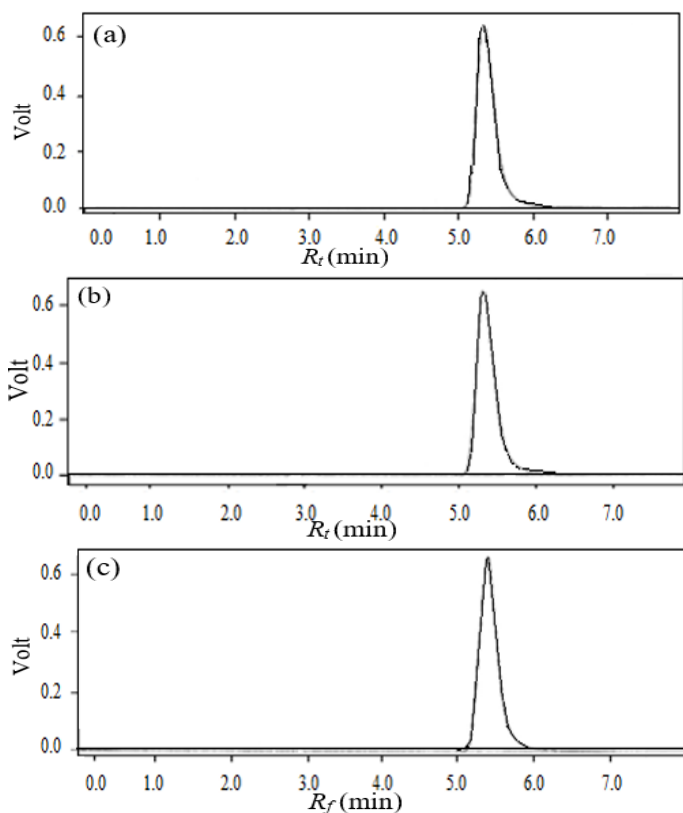


Figure 4. HPLC profiles of the paracetamol samples before and after exposure to radiation and temperature: (a) standard, (b) 40 °C-8 d, (c) UV-12 h, (d) γ -solid, (e) γ -aq, (f) Sun-8 d.

Source: Elaborated by the authors using data from HPLC.

3.4. Scanning electron microscopy (SEM)

Figure 5 displays the images of SEM of paracetamol microparticles before and after having undergone heating to 40 °C temperature and being subjected to UV, sunlight, and γ -ray in both solid and liquid states. The range of particle size for the untreated paracetamol sample is approximately (14.1 – 27.7 μm), and the particles have an irregular crystal form with sharp edges. The morphology of the treated paracetamol particles shows quite distinct alterations. The UV-treated particles exhibit an agglomeration of large rectangular-like particles (19.2 – 49.7 μm) with small ridges growth of the surface ridges. The particles of irradiated by γ -solid have an irregular shape with few small ridges on the surface.

However, the γ -irradiated sample in the aqueous state shows an acicular shape due to the scatter of smaller shape particles.

Exposing the sample to 40 °C for 8 days shows small cylindrical rod-like shape particles with smooth surfaces. The sunlight-irradiated sample has a flakey shape of a very large texture plate.

Although crystallinity from DSC and XRD show few significant changes, SEM images show obvious changes in the morphology and shapes of the treated samples. Some consistency is observed in the particle size from XRD and SEM images.

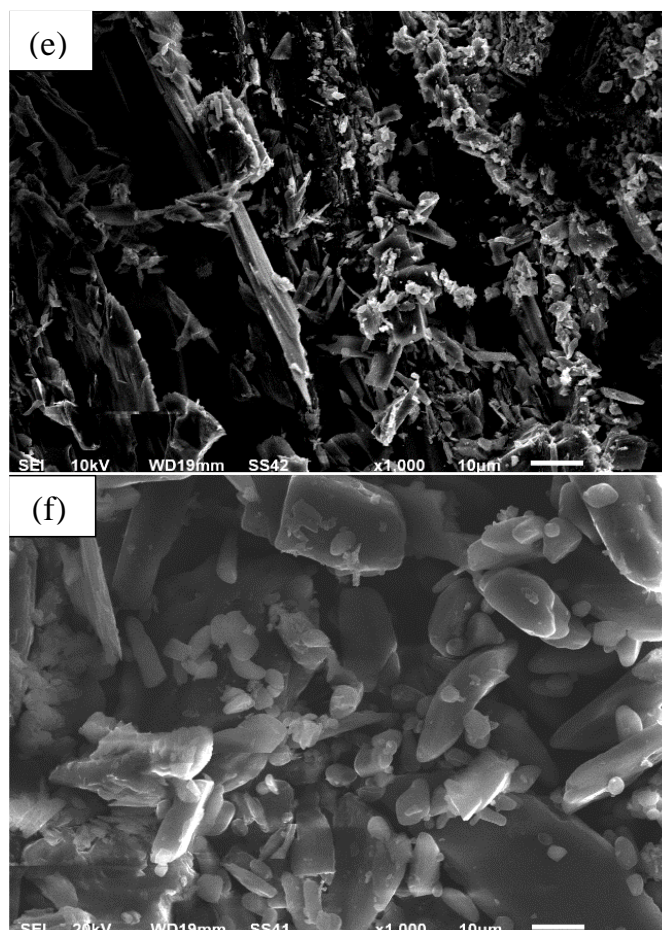
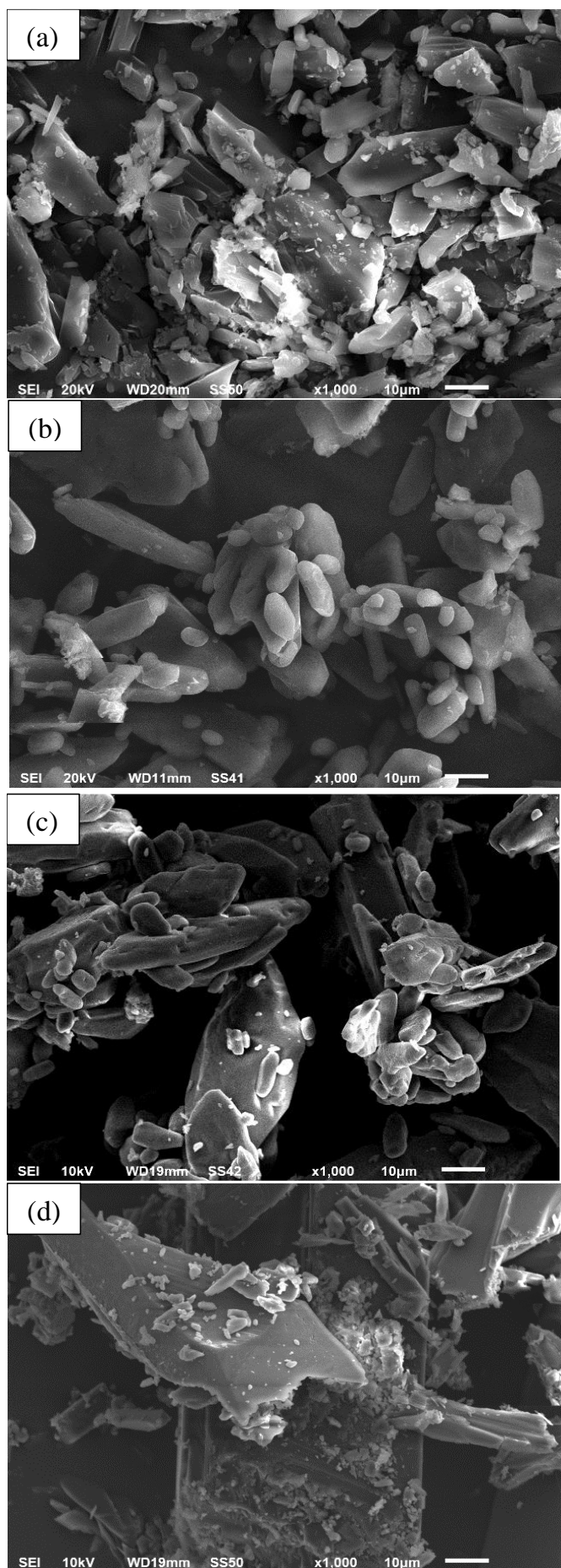


Figure 5. Images of SEM of paracetamol before and after exposure to radiation and temperature: (a) standard, (b) 40 °C-8 d, (c) UV-12 h, (d) γ -solid, (e) γ -aq, (f) Sun-8 d.

Source: Elaborated by the authors using SEM images.

3.5. Photocatalytic decomposition

It is well known that under solar and UV light irradiation, the photocatalytic decomposition of paracetamol (acetaminophen) using a photocatalyst of TiO_2 was conducted, and the efficiency of the process depended on the light intensity. The remaining samples of paracetamol can be removed in aquatic media using this technique (Aguilar *et al.*, 2011; Méndez-Arriaga *et al.*, 2008; Moctezuma *et al.*, 2012; Trujillano *et al.*, 2022).

The kinetic curves of photocatalytic decomposition of paracetamol before and after treatments were evaluated by plotting the concentration (derived from Beer-Lambert law) versus the subjected time. **Figure 6** exhibits the photocatalytic degradation profile of the standard paracetamol and those of the treated samples. The choice of the peaks at $\lambda_{\text{max}} = 254 \text{ nm}$ is intentional because of the apparent generation of the transition that occurs in the benzene ring. The plots of $\ln(C_t/C_0)$ versus t with a variety of initial concentrations of paracetamol samples give straight lines, as in **Fig. 7**. The rate constants of the apparent pseudo-first-order k are investigated by the slopes of linear variations, i.e. (Eq. 7).

$$\ln\left(\frac{C_t}{C_0}\right) = -kt \quad (7)$$

The photocatalytic decomposition of the samples paracetamol before and after treatments is illustrated in **Fig. 6** as influenced significantly by the TiO_2 and sunlight system. The

percentage of degradation is determined from the absorbance spectra by applying the Eq. 8 (Sayan, 2006):

$$\text{Degradation \%} = \frac{C_0 - C_t}{C_0} \times 100 \quad (8)$$

where C_0 is the initial concentration, and C_t is the concentration at a given exposure time.

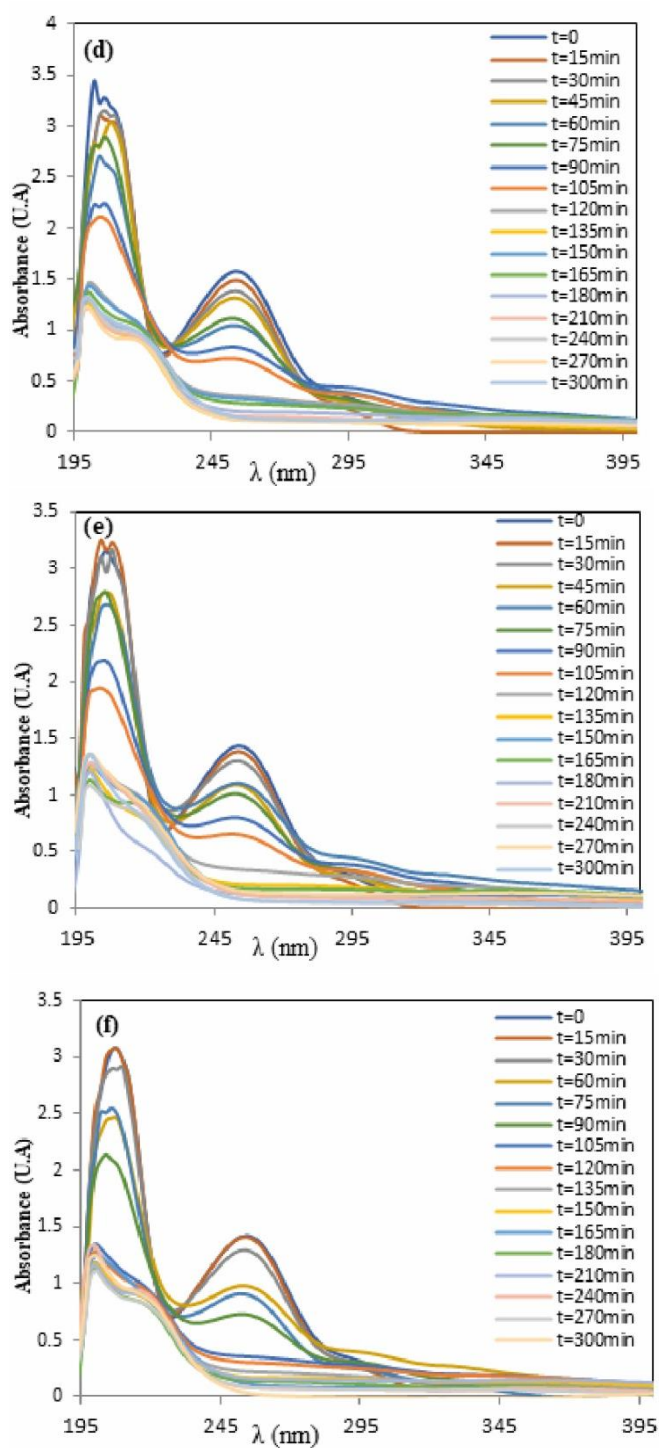
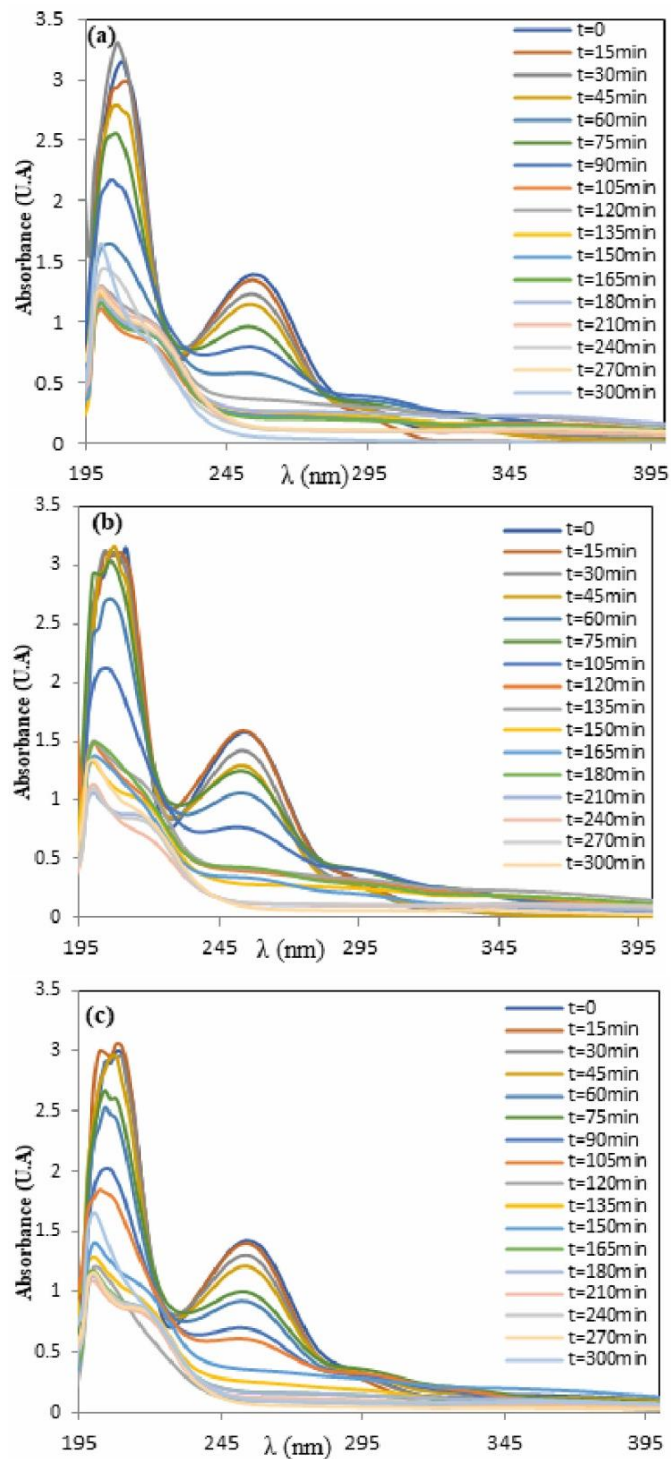


Figure 6. Effect of sunlight on paracetamol before and after exposure to irradiation and temperature: (a) standard, (b) 40 °C-8 d, (c) UV-12 h, (d) γ -solid, (e) γ -aq, (f) Sun-8 d.

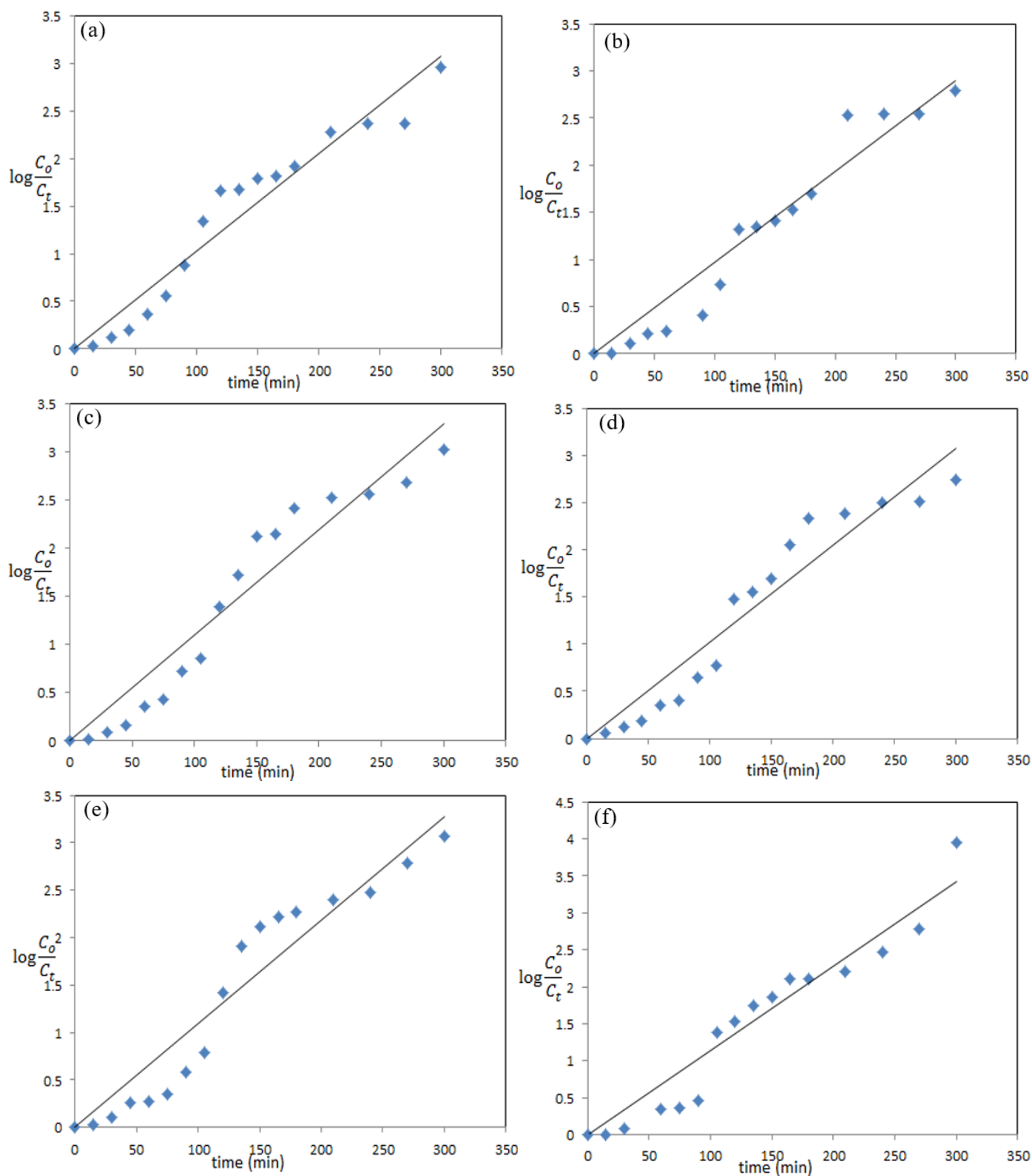


Figure 7. Kinetics of pseudo-first order reaction of the photocatalytic degradation of the paracetamol samples: (a) standard, (b) 40 °C-8 d, (c) UV-12 h, (d) γ -solid, (e) γ -aq, (f) Sun-8 d.

For five hours of sunlight exposure, the decomposition percentage of the samples of paracetamol in Table 4 has been calculated. The variations in the percentage of the decomposition for the paracetamol samples before and after treatments (Table 4)

are not vast. The highest degradation percentage (93.8%) appears for the sample exposed to the temperature of 40 °C, whereas the lowest one (98.1%) is for the sample of sunlight.

Table 4. Half-life, lifetime, rate constant, and percentage of degradation of photocatalytic decomposition of the treated paracetamol.

Paracetamol samples	k (min ⁻¹)	t _{1/2} (min)	R ²	Degradation%	t _{10%} (min)
Standard	0.0102	67.9	0.9417	94.8	10.3
40 °C-8d	0.0097	71.4	0.9433	93.8	10.8
UV-12h	0.0109	63.6	0.9264	95.1	9.6
γ-solid	0.0102	67.9	0.9258	94	10.3
γ-aqueous	0.0109	63.6	0.9176	95.4	9.6
Sunlight	0.0114	60.8	0.9296	98.1	9.2

The half-life of the decomposition of the paracetamol exposed to sunlight exhibits the lower value (60.8 min), whereas the sample treated at 40 °C exhibits the highest value (71.4 min). When a pharmaceutical product is stored under specific conditions, its shelf-life ($t_{10\%}$) is anticipated to be stable or preserve at least 90% of its initial concentration in most circumstances (Carstensen, 1974). It is possible to calculate the photocatalytic decomposition's shelf life from the rate constant by Eq. 9 (Fubara and Notari, 1998):

$$t_{10\%} = \frac{0.105}{k} \quad (9)$$

where $t_{10\%}$ is shelf-life which is the time 10% of the active ingredient of the pharmaceutical product is reduced and k is the rate constant of reaction.

When this equation is applied to the rate constant of photocatalytic decomposition of the samples of standard and treated paracetamol, Table 4 reveals that the shelf-life values dropped dramatically, from 10.8 to 9.2 min. This is because of the influence of TiO₂ catalyst on the decomposition of the samples of paracetamol.

Generally, it has been found that the decomposition percentage has an inverse association with the half-life and shelf-life, indicating that the higher the decomposition percentage, the lower the half-life and shelf-life values.

4. Conclusions

In general, all treated and untreated paracetamol samples undergo a single degradation step. The untreated sample appears to be more thermally stable than the others. Crystallinity from DSC and XRD show few significant changes, however, SEM images exhibit obvious changes in the morphologies and shapes of the treated samples compared to the untreated ones. Some consistency is observed in the particle size from the XRD and the SEM images. HPLC results show almost no purity changes due to chemical degradation associated with the temperature and irradiation treatments. From the outcomes of the photocatalytic degradation, the TiO₂ catalyst proves high efficiency in degrading all the paracetamol samples almost equally (93.8 – 98.1%).

Authors' contributions

Conceptualization: Al-Maydama, H. M.; **Data curation:** Abduljabbar, A. A.; **Formal Analysis:** Abduljabbar, A. A.; **Funding acquisition:** Not applicable; **Investigation:** Al-Maydama, H. M.; **Methodology:** Abduljabbar, A. A.; **Project administration:** Al-Maydama, H. M.; **Resources:** Abduljabbar, A. A.; **Software:** Not applicable; **Supervision:** Al-Maydama, H. M.; **Validation:** Al-Maydama, H. M.; **Visualization:** Abduljabbar, A. A.; **Writing – original draft:** Abduljabbar, A. A.; **Writing – review & editing:** Al-Maydama, H. M.

Data availability statement

The data will be available upon request.

Funding

Not applicable.

Acknowledgments

Not applicable.

References

- Aguilar, C. A.; Montalvo, C.; Ceron, J. G.; Moctezuma, E. Photocatalytic degradation of Acetaminophen. *Int. J. Environ. Health Res.* **2011**, *5* (4), 1071–1078. <https://doi.org/10.22059/IJER.2011.465>
- Akyar, I. *Wide spectra of Quality Control*. In: Tella, A. C.; Salawu, M. O.; Philips, I. M.; Olabemiwo O. M.; and Adediran, G. O. Quality assessment of solid pharmaceuticals and intravenous fluid manufacturing in Sub-Saharan Africa. Intech Open (CCBY 3.0 license. Nigeria) 2011.
- Al-Maydama, H. M.; Abduljabbar, A. A.; Al-Maqtari, M. A.; Naji, K. M. Study of temperature and irradiation influence on the physicochemical properties of Aspirin. *J. Mol. Struct.* **2018**, *1157*, 364–373. <https://doi.org/10.1016/j.molstruc.2017.12.062>
- Al-Maydama, H. M.; El-Shekeil, A. G.; Al-Karbouly, A.; Al-Ikrimawy, W. Thermal degradation behavior of some Poly[4-amino-2,6-pyrimidinodithiocarbamate] metal complexes. *Arab. J. Sci. Eng.* **2009**, *34*(1), 67–75.
- Al-Maydama, H. M. A. Comments on “The effect of UV radiation on the thermal parameters of collagen degradation”. *Polym. Degrad. Stab.* **2004**, *84*, 363–365. <https://doi.org/10.1016/j.polymdegradstab.2003.06.002>
- Boverhof, D. R.; Bramante, C. M.; Butala, J. H.; Clancy, S. F.; Lafranconi, M.; West, J.; Gordon, S. C. Comparative assessment of nanomaterial definitions and safety evaluation considerations. *Regul. Toxicol. Pharmacol.* **2015**, *73*, 137–150. <https://doi.org/10.1016/j.yrtph.2015.06.001>
- British Pharmacopeia, Vol. I & II. Her Majesty's stationary office, London, UK, 2009.
- Carstensen, J. T. Stability of solids and solid dosage forms. *J. Pharm. Sci.* **1974**, *63* (1), 1–14. <https://doi.org/10.1002/jps.2600630103>
- Coats, A. W.; Redfern, J. P. Kinetic parameters from thermogravimetric data. *Nature.* **1964**, *201* (4914), 68–69. <https://doi.org/10.1515/zna-1979-0523>
- Donia, A. M.; Gouda, M. M.; Ayad, M. I.; El-Boraey, H. A. Thermal behavior of some aromatic diamine complexes. *Thermochim. Acta.* **1992**, *194*, 155–163. [https://doi.org/10.1016/0040-6031\(92\)80014-N](https://doi.org/10.1016/0040-6031(92)80014-N)
- Druzhbin, D.; Drebushchak, T.; Min Kov, V.; Boldyneva, E. Crystal structure of two Paracetamol polymorphs at 20 K: A search for the 'structure-property' relationship. *J. Struct. Chem.* **2015**, *52*, 317–323. <https://doi.org/10.1134/S002247661502016X>

- Fubara, O. J. and Notari, R. Influence of pH, temperature, and buffers on Cefepime degradation kinetics and stability predictions in aqueous solutions. *J. Pharm. Sci.* **1998**, *87* (12), 1572–1576. <https://doi.org/10.1021/js980170y>
- Huynh-Ba, K. An Overview of Physical Stability of Pharmaceuticals. In: *Pharmaceutical Stability Testing to Support Global Markets*. 2010, p. 145–152. https://doi.org/10.1007/978-1-4419-0889-6_19
- Jendrzewska, I.; Goryczka, T.; Pietrasik, E.; Klimontko, J.; Jampilek, J. X-ray and Thermal Analysis of Selected Drugs Containing Acetaminophen. *Molecules*. **2020**, *25* (24), 5909. <https://doi.org/10.3390/molecules25245909>
- Lusina, M.; Cindrić, J.; Peko, M.; Pozaić, L.; Musulin, N. Stability study of losartan/hydrochlorothiazide tablets. *Int. J. Pharm.* **2005**, *291*, 127–137. <https://doi.org/10.1016/j.ijpharm.2004.07.050>
- Méndez-Arriaga, F.; Esplugas, S.; Giménez, J. Photocatalytic degradation of non-steroidal anti-inflammatory drugs with TiO₂ and simulated solar irradiation. *Water Research*. **2008**, *42*, 585–594. <https://doi.org/10.1016/j.watres.2007.08.002>
- Moctezuma, E.; Leyva, E.; Aguilar, C. A.; Luna, R. A.; Montalvo, C. Photocatalytic degradation of paracetamol: Intermediates and total reaction mechanism. *J. Hazard. Mater.* **2012**, *243*, 130–138. <https://doi.org/10.1016/j.jhazmat.2012.10.010>
- Oliveira, G. G. G.; Feitosa, A.; Loureiro, K.; Fernandes, A. R.; Souto, E. B.; Severino, P. Compatibility study of paracetamol, chlorpheniramine maleate and phenylephrine hydrochloride in physical mixtures. *Saudi Pharmaceutical Journal*. **2017**, *25* (1), 99–103. <https://doi.org/10.1016/j.sjps.2016.05.001>
- Prime, R. B.; Bair, H. E.; Vyazovkin, S.; Gallagher, P. K.; Riga, A. *Thermogravimetric analysis (TGA)*. In: *thermal analysis of polymers: Fundamentals and Applications*, eds. J. D. Menczel and R. B. Prime. Hoboken: Wiley, 2009. <https://doi.org/10.1002/9780470423837.ch3>
- Şayan, E. Optimization, and modeling of decolorization and COD reduction of reactive dye solutions by ultrasound-assisted adsorption. *Chem. Eng. J.* **2006**, *119*, 175–181. <https://doi.org/10.1016/j.cej.2006.03.025>
- Schnitzler, E.; Lençone, K.; Kobelnik, M. Characterization of pharmaceuticals by thermal analysis. *Ciências Exatas e da Terra, C. Agrárias e Engenharias*. **2002**, *8*(1), 91–100.
- Suno, M.; Ichihara, H.; Ishino, T.; Yamamoto, K.; Yoshizaki, Y. Photostability studies on (±)-tramadol in a liquid formulation. *J. Pharm. Health Care Sci.* **2015**, *1* (5), 1–6. <https://doi.org/10.1186/s40780-014-0003-2>
- Tomassetti, M.; Catalanib, A.; Rossib, V.; Vecchio, S. Thermal analysis study of the interactions between acetaminophen and excipients in solid dosage forms and in some binary mixtures. *J. Pharm. Biomed. Anal.* **2005**, *37*, 949–955. <https://doi.org/10.1016/j.jpba.2004.10.008>
- Trujillano, R.; Rives, V.; García, I. Photocatalytic Degradation of Paracetamol in Aqueous Medium Using TiO₂ Prepared by the Sol-Gel Method. *Molecules*. **2022**, *27* (9), 2904. <https://doi.org/10.3390/molecules27092904>
- Varshny, L. and Patel, K. M. Effects of ionizing radiation on the pharmaceutical compound, Chloramphenicol. *Radiat. Phys. Chem.* **1994**, *43* (5), 471–480. [https://doi.org/10.1016/0969-806X\(94\)90064-7](https://doi.org/10.1016/0969-806X(94)90064-7)
- Vermeire, A.; Remon, J. P. Stability and compatibility of morphine: Review. *Int. J. Pharm.* **1999**, *187*, 17–51. [https://doi.org/10.1016/S0378-5173\(99\)00181-7](https://doi.org/10.1016/S0378-5173(99)00181-7)
- Yousaf, M.; Nazir, S.; Hayat, Q.; Akhtar, M. N.; Akbar, M.; Lu, Y.; Noor, A.; Zhang, J.; Shah, M.A.K.; Wang, B. Magneto-optical properties and physical characteristics of M-type hexagonal ferrite (Ba_{1-x}Ca_xFe_{11.4}Al_{0.6}O₁₉) nanoparticles (NPs). *Ceram. Int.* **2021**, *47* (8), 11668–11676. <https://doi.org/10.1016/j.ceramint.2021.01.006>